Struct Multidisc Optim (2010) 41:735–747
DOI 10.1007/s00158-009-0444-7

INDUSTRIAL APPLICATION

A level set based method for the optimization of cast part

Qi Xia · Tielin Shi · Michael Yu Wang · Shiyuan Liu

Received: 21 March 2009 / Revised: 24 September 2009 / Accepted: 24 September 2009 / Published online: 28 October 2009

Abstract A cast part is formed via casting process in which molten liquid is poured into and solidifies in a cavity enclosed by molds. Then, one obtains the cast part when the molds are removed. An important issue in the casting process is that a cast part should have a proper geometry so that the molds can actually be removed. Accordingly, in the optimization of a cast part one not only needs to optimize the performance of the cast part but also needs to ensure the cast part have a proper geometry. With these goals, a level set based method is proposed for the optimization of cast part. A molding condition and a performance condition on the design velocity are derived for the optimization. Numerical examples are provided in 2D and 3D.

Keywords Structure optimization · Level set · Cast part · Molding constraint

1 Introduction

Optimization is an effective tool for obtaining high performance structures. During the past decades size optimization, shape optimization, and topology optimization have been extensively developed. While the performance of a structure can be improved via the optimization, another aspect in the design of a structure—manufacturing—also needs to be carefully treated. Specifically, a structure should be designed in a way that it can be easily manufactured via intended techniques. A cast part considered in this paper is a structure intended to be manufactured via casting process.

In the casting process molten liquid is poured into and solidifies in a cavity enclosed by molds, and one obtains the cast part when the molds are removed. An important issue in the casting process is that a cast part should have a proper geometry so that the molds can be removed, or the so-called molding constraint can be satisfied. Therefore, the optimization of a cast part should not only optimize the performance of the cast part but also should ensure the cast part have a proper geometry.

Much effort has been made for incorporating the molding constraint of casting process into structure optimization, in particular the topology optimization. TopShape (Baumgartner et al. 1992; Mattheck 1990; Harzheim and Graf 1995), a program developed at the International Development Center of Adam Opel and based on CAO (Computer Aided Optimization) and SKO (Soft Kill Option) (Baumgartner et al. 1992; Mattheck 1990; Harzheim and Graf 1995), is the first program that successfully incorporated the molding constraint of casting process into topology optimization (Harzheim and Graf 2002, 2005, 2006). Several topology control algorithms (connectivity control, growth direction control, thickness control, et al.) were introduced in the TopShape. Based on the SIMP (Solid Isotropic Microstructure with Penalization) method (Bendsøe 1989; Rozvany et al. 1992; Bendsøe and Sigmund 2003), Zhou et al. proposed a mathematical formulation of the molding constraint that constraints the material densities in the lower positions to be bigger than those in the

Q. Xia (✉) · S. Liu
The State Key Laboratory of Digital Manufacturing Equipment and Technology, Huazhong University of Science and Technology, Wuhan, China
e-mail: xiaqi.hust.cn@gmail.com

T. Shi
Wuhan National Laboratory for Optoelectronics, Wuhan, China

M. Y. Wang
Department of Mechanical and Automation Engineering,The Chinese University of Hong Kong, Shatin, New Territories, Hong Kong

upper positions (Zhou et al. 2001). This approach is available in OptiStruct (Altair Engineering, Inc. 2002). Leiva et al. proposed a novel design parametrization that explicitly incorporates growth direction into its design variables for the topology optimization of cast part (Leiva et al. 2004a, b) and implemented it in GENESIS (Leiva et al. 1999).

Also, much effort has been made in optimal control of casting process, since shrinkage cavity in a cast part, residual stresses in a cast part, and the production costs all depend on the casting process. Tortorelli et al. proposed the optimal design of nonlinear parabolic systems (Tortorelli et al. 1994) and applied it to the control of casting process (Morthland et al. 1995; Ebrahimi et al. 1997). Lewis et al. proposed an optimization procedure to determine the optimum size, location and number of feeders and chills in the sand casting process (Lewis et al. 2001). Tavakoli and Davami used the SIMP method to optimize the riser to prevent hot-spot danger in the sand casting process (Tavakoli and Davami 2008).

In our present study, we do not consider the optimization of casting process but focus on the optimal design of the cast parts. Specifically, we propose a level set based method for the optimization of cast parts by which both the performance of the cast parts and the molding constraint are addressed.

The paper is organized as follows. A brief introduction to casting process is given at the beginning. Then, the implicit representation of a structure via level set model is presented. Thereafter, the molding condition on the design velocity are described. Next, formulation of the optimization problem is given and the performance condition on the design velocity is derived based on shape derivative. Details of implementation and numerical examples are provided next. Conclusions are given in the end.

2 A brief introduction to casting process

In our present study, we consider the casting process that uses two molds (the two molds are removed in opposite directions). As aforementioned, an important issue in the casting process is that a cast part should have a proper geometry so that the molds can be removed, or the so-called molding constraint can be satisfied. Examples of the cases where the molds can be and cannot be removed are given in Fig. 1a and b, respectively. In Fig. 1b, the lower mold is stuck by a slot called undercut and cannot be removed in the given direction. The direction in which a mold is removed is called the parting direction, and the surface where the two molds contact each other is called the parting surface.

We observe that with the casting process described above a cast part should not have any undercut as shown in the Fig. 1b. Besides, another requirement on a cast part is that the cast part should not have any interior void, i.e., a region completely contained in the interior of a solid, since such interior void cannot be manufactured by casting process. Therefore, we have the following conclusion: with the casting process considered in the present study a cast part is required to have no undercut and no interior void.

Another understanding of the above conclusion can be described as follows. If a structure has no undercut and no interior void, and given with two opposite parting directions $\mathbf{d}$ and $-\mathbf{d}$, the surface Γ of the structure can be divided into two disjoint pieces Γ_1 and Γ_2 ($\Gamma_1 \cap \Gamma_2 = \emptyset$, $\overline{\Gamma_1 \cup \Gamma_2} = \Gamma$) such that Γ_1 can be parted in the direction $\mathbf{d}$, and Γ_2 can be parted in the direction $-\mathbf{d}$. A moldability condition for the two pieces of the structure's surface can given as follows, according to Reference (Fu et al. 2002):

$$\begin{cases} \mathbf{d} \cdot \mathbf{n}(x) \geq 0, & \forall x \in \Gamma_1 \\ \mathbf{d} \cdot \mathbf{n}(x) \leq 0, & \forall x \in \Gamma_2 \end{cases} \tag{1}$$

where $\mathbf{n}$ is the outward unit normal to the surface.

3 The level set method

Level set method, first introduced by Osher and Sethian (1988), is a method for numerical simulation of motion of interfaces in two or three dimensions. It has caught extensive attentions in the topology optimization of continuum

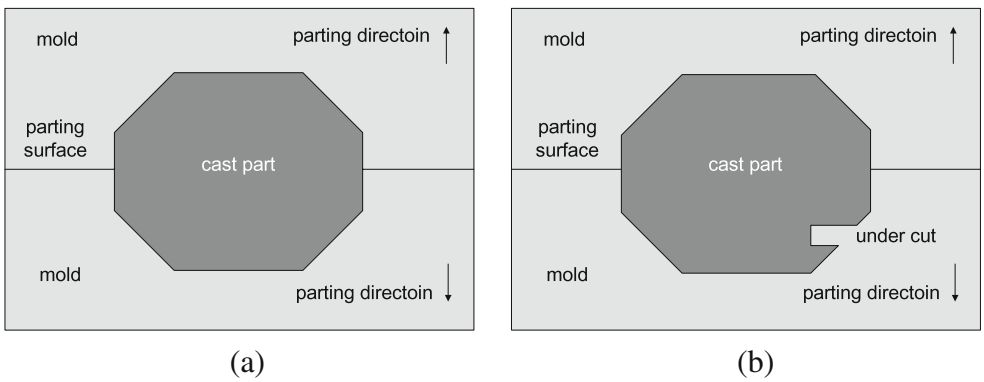

Fig. 1 Examples of the cases where the molds can be and cannot be removed. **a** Molds can be removed. **b** Molds cannot be removed

structures since the seminal papers (Sethian and Wiegmann 2000; Osher and Santosa 2001; Allaire et al. 2002, 2004; Wang et al. 2003).

Let $\Omega \subseteq \mathbb{R}^{\mathrm{d}}(\mathrm{d} = 2, 3)$ be the region occupied by a structure. The level set model specifies the boundary Γ in an implicit form as the zero level set of a one-higher dimensional scalar function, $\Phi : \mathbb{R}^{\mathrm{d}} \to \mathbb{R}$,

$$\Gamma = \{x \mid \Phi(x) = 0\}$$

Then the design domain $\mathcal{D}$ is partitioned according to the following rule:

$$\begin{aligned} \Phi(\mathbf{x}) = 0 &\iff \forall\, \mathbf{x} \in \partial\,\Omega \cap \mathcal{D} \\ \Phi(\mathbf{x}) < 0 &\iff \forall\, \mathbf{x} \in \Omega \backslash \partial\Omega \\ \Phi(\mathbf{x}) > 0 &\iff \forall\, \mathbf{x} \in (\mathcal{D} \backslash \Omega) \end{aligned}$$

where $\mathcal{D} \subset \mathbb{R}^{\mathrm{d}}$ is a fixed design domain in which all admissible shapes Ω are included, i.e. $\Omega \subseteq \mathcal{D}$. In the level set method, the scalar function Φ is generally constructed to be a signed distance function ($|\nabla\Phi| \equiv 1$) to the boundary. With such a signed distance function, the unit outward normal $\mathbf{n}$ to the boundary is given by $\mathbf{n} = \nabla\Phi$.

Propagation of the free boundary of a structure in the optimization process is described by the Hamilton-Jacobi equation:

$$\frac{\partial \Phi}{\partial t} + \mathbf{V} \cdot \mathbf{n} = 0 \tag{2}$$

where $\mathbf{V}$ is the velocity vector defined on the boundary Γ, as illustrated in Fig. 2. The velocity is an important link between the level set method and an optimization algorithm (Wang et al. 2003), and it is usually called the design velocity. A proper variation of the free boundary of a structure is obtained as a descent direction of an objective function via sensitivity analysis. Then, such boundary variation is treated as the velocity $\mathbf{V}$ in the Hamilton-Jacobi equation.

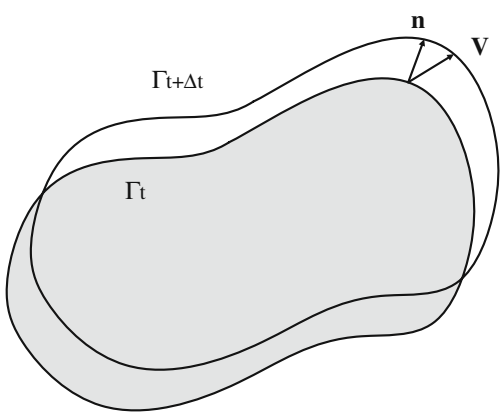

Fig. 2 The velocity and the propagation of a boundary

An important property of the Hamilton-Jacobi equation is that it satisfies the maximum principle. As a result, voids cannot be nucleated in the interior of a structure (Allaire et al. 2004). This makes the level set based topology optimization, especially in 2D, depend on the initial design. To overcome this dependence much effort has been made for incorporating topological derivative (Sokolowski and Zochowski 1999) into the level set based topology optimization (Allaire and Jouve 2006; Burger et al. 2004; He et al. 2007). But, in the context of optimization of cast part, since it is required that a cast part should not have any interior void, the lack of void nucleation in the level set based method actually appears as an advantage for this specific application.

4 Molding condition on design velocity

Suppose that the optimization starts with an initial design that has no interior void and no undercut, i.e., a design satisfying the moldability condition (1), how can we ensure the resulting structure also have no interior void and no undercut, or still satisfying (1)? This is the question to be answered in this section. Our idea is to restrict the boundary motion during the optimization, which leads to the "molding condition" on the design velocity described as follows.

Molding Condition For a cast part that is to be manufactured with two molds and the two molds are removed in directions $\mathbf{d}$ and $-\mathbf{d}$, respectively, and if the optimization starts from an initial design that is moldable with respect to the parting directions, it will be sufficient to have a castable design if the design velocity vector has the following form:

$$\mathbf{V}(x) = \lambda(x)\,\mathbf{d}, \quad \forall x \in \Gamma \tag{3}$$

where λ is a real number.

According to (3) any point on the free boundary of a structure is made to move in the parting directions $\mathbf{d}$ (when $\lambda(x) > 0$) or $-\mathbf{d}$ (when $\lambda(x) < 0$), and when $\lambda = 0$ the point dose not move. Therefore, the motion of any point on the structure boundary is restricted to have no component in the direction orthogonal to the parting directions $\mathbf{d}$ and $-\mathbf{d}$. Now let's see how this restricted motion can ensure the molding constraint be satisfied.

As aforemention, an interior void can not be *nucleated* in the level set method, but it is indeed possible that when two pieces of structural boundary partially merge together, they can *enclose* a void right in the interior of the structure, as illustrated in Fig. 3. Fortunately, it can be verified that such enclosing of interior void can be prevented by the restricted motion given by (3).

For the problem of undercut, more explanation is needed. First, when a cast part is optimized without a pre-selected

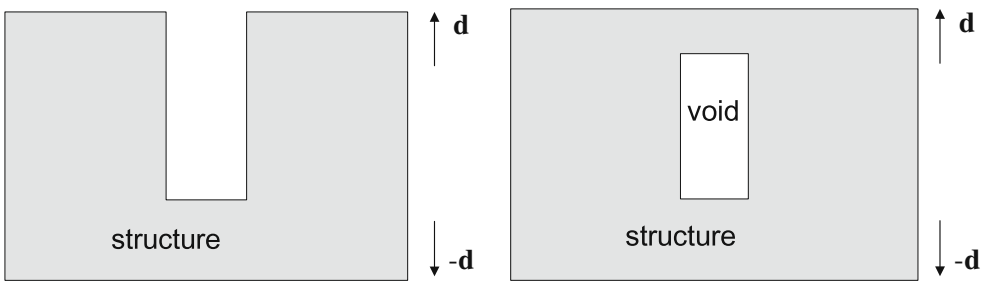

Fig. 3 An interior void is enclosed when two pieces of boundary partially merge together. **a** A structure without interior void. **b** A structure with an enclosed interior void

parting surface, the restricted motion of the boundary given by (3) is enough to prevent the undercut from emerging during the optimization, since the restricted motion can not change a point that is visible from the parting directions to be invisible. If there is no pre-selected parting surface, the parting surface of the cast part obtain by optimization needs to be computed after the optimization via the methods developed for computed aided mold design (Fu et al. 2002; Ahn et al. 2002; Li et al. 2007). Such computed parting surface may be planar or not planar. In practical engineering applications, a simple planar parting surface is more preferable because it reduces the costs of mold fabrication and the complexity of mold operation (Ravi and Srinivasan 1990; Majhi et al. 1999). Therefore, it is attractive to do the optimization of cast parts with a simple pre-selected planar parting surface. In this case, more effort is needed to prevent the undercut from emerging during the optimization.

With a pre-selected planar parting surface, the design domain $\mathcal{D}$ is separated to two sub-domains: $\mathcal{D}_1$ and $\mathcal{D}_2$, as shown in Fig. 1a. Also, the boundary Γ of an initial design is separated to two parts: $\Gamma_1 \subset \mathcal{D}_1$, $\Gamma_2 \subset \mathcal{D}_2$, and $\overline{\Gamma_1 \cup \Gamma_2} = \Gamma$, $\Gamma_1 \cap \Gamma_2 = \emptyset$. In order to prevent the undercut that would stick the mold, as illustrated in Fig. 4, we let Γ_1 and Γ_2 propagate independently in $\mathcal{D}_1$ and $\mathcal{D}_2$ according to the restricted motion. In other word, Γ_1 is confined to the sub-domain $\mathcal{D}_1$ and can not be propagated across the parting surface. The situation for Γ_2 is similar.

A fact worthy notice is that if a design velocity complies with (3), then during the optimization a structure can shrink but cannot expand in the directions orthogonal to the parting directions, therefore it's preferable to start the optimization from an initial design that has the biggest extent in the direction orthogonal to the parting directions.

To conclude, if the optimization starts with an initial design that has no interior void and no undercut, and if the boundary motion is restricted by the molding condition, the resulting structure is ensured to have no interior void and no undercut, thus can be manufactured by the casting process considered in the present study. According to (1), the molding condition on the design velocity based on (3) can be considered as a sufficient (but not essentially a necessary) moldability constraint.

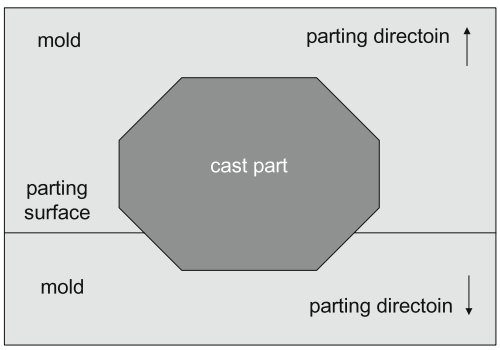

Fig. 4 The upper mold can not be removed in the parting direction

5 The performance condition on design velocity

In this section we present the related formulations of a linear elastic structure, the formulation of minimum compliance optimization problem, and a performance condition on the design velocity derived based on shape derivative.

The weak form of the equation of a linear elastic structure is

$$a(\mathbf{u}, \mathbf{v}) = \ell(\mathbf{v}), \quad \forall \mathbf{v} \in \mathbf{U} \tag{4}$$

with $\mathbf{U}$ denoting the space of kinematically admissible displacement fields, and

$$a(\mathbf{u}, \mathbf{v}) = \int_\Omega \mathbf{E}_{ijkl}\, \varepsilon_{kl}(\mathbf{u})\, \varepsilon_{ij}(\mathbf{v})\, \mathrm{d}\Omega$$

$$\ell(\mathbf{v}) = \int_\Omega \mathbf{f}_i\, \mathbf{v}_i \mathrm{d}\Omega + \int_{\Gamma_N} \mathbf{t}_i\, \mathbf{v}_i \mathrm{d}\Gamma$$

where $\mathbf{E}$ is the elasticity tensor; the strain tensor $\boldsymbol{\varepsilon}$ is defined by linear strain-displacement relation $\varepsilon_{kl} = \frac{1}{2}(\mathbf{u}_{k,l} + \mathbf{u}_{l,k})$; $\mathbf{u}$ is the displacement field; $\mathbf{f}$ is the body force; $\mathbf{t}$ is the traction force.

The minimum compliance optimization problem is defined as:

$$\text{Minimize} \quad J(\Omega) = \ell(\mathbf{u}, \Omega) \tag{5}$$

$$\text{Subject to :} \quad a(\mathbf{u}, \mathbf{v}) = \ell(\mathbf{v}), \quad \forall \mathbf{v} \in \mathbf{U} \tag{6}$$

$$\int_{\Omega} \mathrm{d}\Omega \leq \overline{V} \tag{7}$$

where the objective function $J(\Omega)$ accounts for the work done by external forces and also characterizes the stiffness of a structure. The constraint (7) is utilized to put a limit on material resource, i.e. its volume, where $\overline{V}$ is the upper bound of the volume of material allowed for the structure.

Assuming there exists no body force ($\mathbf{f} \equiv 0$), and noticing that the only part of a structure's boundary subject to optimization is the traction free boundary Γ_H (Allaire et al. 2004), the shape derivative is obtained based on local perturbations as Allaire et al. (2004):

$$J' = \int_{\Gamma_H} G\,\mathbf{n} \cdot \mathbf{V}\,\mathrm{d}\Gamma, \quad G = \Lambda - \mathbf{E}_{ijkl}\,\boldsymbol{\varepsilon}_{kl}(\mathbf{u})\,\boldsymbol{\varepsilon}_{ij}(\mathbf{u}) \tag{8}$$

where $G\mathbf{n}$ is the so-called shape gradient; G is the shape gradient density; and Λ is a Lagrange multiplier for the volume constraint, i.e., (7). Several techniques can be employed to determine the Lagrange multiplier: the augmented Lagrange multiplier method (Nocedal and Wright 1999), fixed Lagrange multiplier (Allaire et al. 2004), boundary integration method (Wang et al. 2003). In the present work we employ the augmented Lagrange multiplier method.

According to the shape derivative given in (8), we can readily define a "performance condition" on the design velocity $\mathbf{V}$ which amounts to choosing a descent direction.

Performance Condition The objective function decreases if the design velocity V satisfies the following inequality and if the boundary is propagated according this design velocity with a monotone line-search or small step size

$$G(x)\,\mathbf{n}(x) \cdot \mathbf{V}(x) \leq 0, \ \forall x \in \Gamma_H \tag{9}$$

It can be readily seen that this particular velocity $\mathbf{V}$ yields $J' \leq 0$ which implies the descent of the objective function.

6 The design velocity for the optimization of cast parts

In Sections 4 and 5 we obtained the molding condition and the performance condition on the design velocity, respectively. The former offers a tool to ensure a structure have a proper geometry so that it can be manufactured by the casting process considered in the present study. The latter offers a guidance for choosing a design velocity to improve a structure's performance, i.e., the stiffness in the present study. In this section, we combine the two conditions and arrive at the design velocity that is used for the optimization of cast part.

Such a combination is given by the following equation,

$$\mathbf{V}(x) = -\mathrm{sign}(\mathbf{n} \cdot \mathbf{d})\, G\,\mathbf{d} = \begin{cases} G\,\mathbf{d}, & \mathbf{n} \cdot \mathbf{d} \leq 0 \\ -G\,\mathbf{d}, & \mathbf{n} \cdot \mathbf{d} > 0 \end{cases}, \ \forall x \in \Gamma_H \tag{10}$$

It is easy to verify that the design velocity given by (10) indeed conforms to the the molding condition given by (3). When $\mathbf{n} \cdot \mathbf{d} \leq 0$, the λ in (3) is equal to G, and when $\mathbf{n} \cdot \mathbf{d} > 0$, the λ in (3) is equal to $-G$.

In order to check whether the design velocity given by (10) can reduce the objective function, we substitute (10) into (8) and obtain

$$J' = \int_{\Gamma_H^1} (G\,\mathbf{n} \cdot G\,\mathbf{d})\,\mathrm{d}\Gamma \ - \int_{\Gamma_H^2} (G\,\mathbf{n} \cdot G\,\mathbf{d})\,\mathrm{d}\Gamma \tag{11}$$

where $\Gamma_H^1 = \{x \,|\, \mathbf{n}(x) \cdot \mathbf{d} \leq 0, \ x \in \Gamma_H\}$, $\Gamma_H^2 = \{x \,|\, \mathbf{n}(x) \cdot \mathbf{d} > 0, \ x \in \Gamma_H\}$. From (11) we see that the shape derivative is non-positive, i.e., $J' \leq 0$, which implies descent of the objective function. After the above analysis, we can see that the design velocity selected according to (10) is appropriate for the optimization of cast part.

7 Implementation

In this section we describe the implementation of the level set based method for the optimization of cast parts. In particular we will describe velocity extension, numerical solution to the Hamilton-Jacobi (HJ) equation, reinitialization, and implementation of the finite element method.

7.1 Velocity extension

It should be noted that in the level set based method the design velocity $\mathbf{V}$ defined on the free boundary of a structure must be extended to the whole design domain $\mathcal{D}$ or a narrow band around the free boundary (Osher and Sethian 1988; Sethian 1999). There are many approaches to construct the extension velocity (Sethian 1999; Ye et al. 2002). In the optimization of continuum structures, since a fixed finite element mesh is used for the finite element analysis, and voids are represented by weak material, the design velocity which is defined on the traction free boundary Γ_H can be naturally extended to the entire design domain D as $\mathbf{V}^e = \mathbf{V}, \ \forall x \in \mathcal{D}$. Therefore, in the present study,

the design velocity is extended to the entire design domain $\mathcal{D}$ as:

$$\mathbf{V}^e(x) = \begin{cases} -\text{sign}(\mathbf{n}\cdot\mathbf{d})\, G(x)\, \mathbf{d} & \forall\, x \in \Xi \\ -\text{sign}(\mathbf{n}\cdot\mathbf{d})\, \Lambda\, \mathbf{d} & \forall x \in \mathcal{D}\backslash\Xi \end{cases} \tag{12}$$

where $\Xi = \left\{x \in \mathbb{R}^d \mid |\Phi(x)| \leqslant \delta\right\}$ is a narrow band around Γ_H. The width δ of the narrow band is set to be twice the grid size.

The reason for using the above velocity extension instead of a more accurate one is described as follows. The velocity extension methods developed in the major literature are primarily for an accurate propagation of an interface. The nature of the problem of structure optimization, however, is very different since our goal is to find the optimal shape in an efficient manner. Accurate structure shape in the intermediate steps of optimization is of no practical significance as long as the final solution obtained is at the global or local minimum of the objective function.

7.2 Numerical solution to HJ equation

With $\mathbf{V}^e$ given by (12), the HJ equation (2) contains only the first order derivatives of Φ, which leads to a hyperbolic type of PDE (Sethian 1999; Osher and Fedkiw 2002). A variety of spatial and time discretization schemes were devised to solve this type of PDE. In the present implementation, we employ the forward Euler time discretization and the 1st-order upwind spatial discretization:

$$\begin{aligned}\Phi_{ijk}^{n+1} = \Phi_{ijk}^n - \Delta t\, [\, &\max(u_{ijk}^n, 0)\, D_{ijk}^{-x} + \min(u_{ijk}^n, 0)\, D_{ijk}^{+x} \\ &+\max(v_{ijk}^n, 0)\, D_{ijk}^{-y} + \min(v_{ijk}^n, 0)\, D_{ijk}^{+y} \\ &+\max(w_{ijk}^n, 0)\, D_{ijk}^{-z} + \min(w_{ijk}^n, 0)\, D_{ijk}^{+z}\,]\end{aligned} \tag{13}$$

where Φ_{ijk}^n is the value of Φ at time step n, grid point (i, j, k); $(u_{ijk}^n, v_{ijk}^n, w_{ijk}^n)$ is the velocity; D_{ijk}^{-x}, D_{ijk}^{+x}, D_{ijk}^{-y}, D_{ijk}^{+y}, D_{ijk}^{-z}, D_{ijk}^{+z} are the backward and forward finite difference of Φ along x, y, and z axis, respectively. Δt should satisfy the CFL (Courant-Friedreichs-Lewy) stability condition:

$$\Delta t \max\left\{\frac{|u|}{\Delta x} + \frac{|v|}{\Delta y} + \frac{|w|}{\Delta z}\right\} < \alpha, \quad 0 < \alpha < 1$$

7.3 Reinitialization

Since the level set function Φ often becomes too flat or too steep during the optimization which leads to increasing numerical error, a reinitialization procedure is periodically performed to restore Φ to a signed distance function to the free boundary of a structure (Sethian 1999; Osher and Fedkiw 2002). That is, to restore $|\nabla\Phi| = 1$. Such a reinitialization can be achieved by solving the following PDE:

$$\frac{\partial\Phi}{\partial t} + \text{sign}(\Phi_0)\,(|\nabla\Phi| - 1) = 0 \tag{14}$$

where Φ_0 is the initial hypersufface. Numerical solutions to (14) can be found in Ref. (Sussman et al. 1994; Peng et al. 1999; Osher and Fedkiw 2002). In the present study we employed the method of Ref. (Peng et al. 1999).

7.4 Finite element method

In the present study, Eulerian-type methods employing fixed mesh and artificial weak material is adopted as the finite element analysis (FEA) tool (Allaire et al. 2004; Wang et al. 2003). In this method, instead of solving the state equation on structure Ω, we solve it on the entire design domain $\mathcal{D}$ with the void $\mathcal{D}\backslash\Omega$ being represented by weak material. The material properties of the weak material is tailored so that the results of FEA obtained on the entire design domain $\mathcal{D}$ is consistent to that obtained on the structure $\Omega \subset \mathcal{D}$.

8 Numerical examples

In this section the proposed level set based method is applied to several examples in two dimensions and three dimensions. In these examples, it is assumed that the solid material has a Young's modulus $E = 1$ and Poisson's ratio $\nu = 0.3$, the weak material has a Young's modulus $E = 0.001$ and Poisson's ratio $\nu = 0.3$. For all examples, a fixed mesh of 4-node bilinear square elements are used in 2D and 8-node trilinear cube elements are used in 3D for the finite element analysis. In the computation of level set, reinitialization is performed in every iteration of optimization.

8.1 2D examples

The main purpose of the 2D examples is to show the effect of the molding condition, since 2D structures are rarely manufactured by casting. The design problem of a 2D short

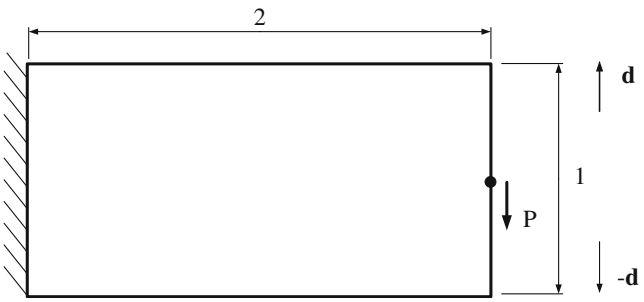

Fig. 5 The design problem of a 2D cantilever beam

cantilever beam is shown in Fig. 5. The entire design domain $\mathcal{D}$ is a rectangle of size 2×1 with a fixed boundary on the left side and a unit vertical point load $P = 1$ is applied at the middle point of the right side. The $\mathbf{d}$ and $-\mathbf{d}$ are the parting directions. The volume of material allowed for the structure is 40% of the design domain.

Firstly, we consider the optimization of the cast part without a pre-selected parting surface. An 80×40 mesh is used for the finite element analysis. An 81×41 rectilinear grid is used for level set computations. The initial design that has no interior void and undercut is shown in Fig. 6a. Beginning with such an initial design, the optimization gives the optimal structure shown in Fig. 6b. Since the parting directions are along the y-axis, the motion of points on the structure boundary is restricted to be along the y-axis, therefore undercuts are prevented. The optimization in this example is in fact a shape optimization but not topology optimization, since no topology changes occurred during the optimization.

Secondly, we consider the optimization of the cast part with a pre-selected parting surface. Figure 6c shows the initial design and the pre-selected planar parting surface shown by the dash line. The height of the sub-domain $\mathcal{D}_2$ below the parting surface is 0.675. An 80×40 mesh is used for the finite element analysis. An 81×14 rectilinear grid is used for level set computations in the upper sub-domain, and an 81×27 rectilinear grid is used for level set computations in the lower sub-domain. In order to deal with the pre-selected parting surface, the Φ is separated to Φ_1 in the upper sub-domain and Φ_2 in the lower sub-domain. The Φ_1 and Φ_2 are updated independently. The resulting optimal structure is shown in Fig. 6d. Also, the optimization in this example is a shape optimization.

Finally, the design problem is solved via optimization without considering the molding constraint of casting process. The initial design and the corresponding optimal structure are shown in Fig. 6e and f, respectively.

From the numerical results described in the caption of Fig. 6, we can see that the compliance of the optimal structure obtained without molding constraint is much smaller than those obtained with molding constraint. The reason of this fact is obvious. The restricted motion behaves like a constraint of the optimization and restricts the flexibility of the boundary evolution thus restricts the design space of the optimization.

8.2 3D examples

In this section, we consider a design problem in 3D, shown in Fig. 7. The design domain is a parallelepiped of size

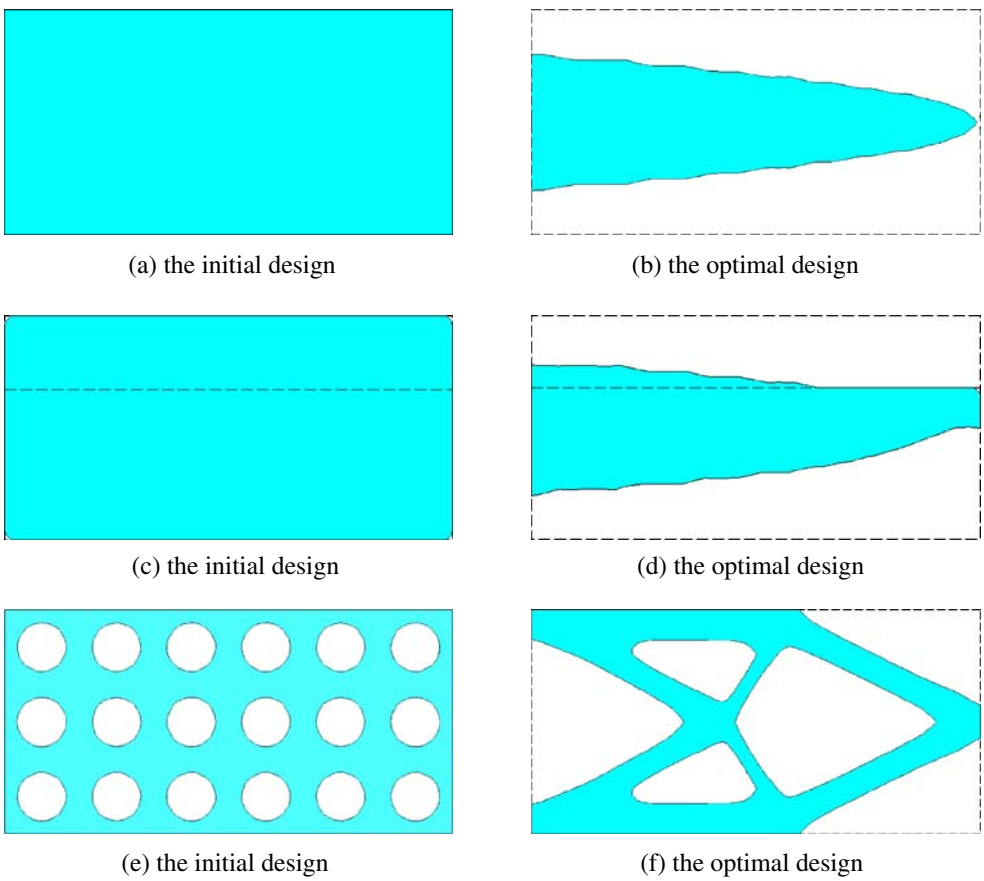

(a) the initial design (b) the optimal design

(c) the initial design (d) the optimal design

(e) the initial design (f) the optimal design

Fig. 6 Optimization of cast parts in 2D. **a**, **b**: optimization of a cast part without a pre-selected parting surface, in the optimal design the material volume is 39.80% and compliance is 323.57; **c**, **d**: optimization of a cast part with a pre-selected parting surface, in the optimal design the material volume is 40.37% and compliance is 314.99; **e**, **f**: optimization without considering molding constraint, in the optimal design the material volume is 40.05% and compliance is 73.97

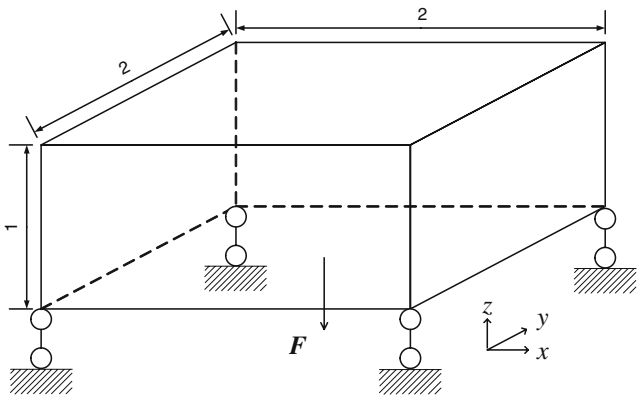

Fig. 7 The design problem in 3D

$2 \times 2 \times 1$ with the four corners at the bottom face being fixed along the z axis and being free along the x and y axis. A unit vertical point load $F = 1$ is applied at the center of the bottom face. Because of the symmetry of the design domain and load, only a quarter is considered in the computations. Moreover, if the design domain of this example is considered as a whole in the finite element analysis, the stiffness matrix would be singular. The quarter domain is discretized by $20 \times 20 \times 20$ tri-linear 8-node cube elements for finite element analysis. A $21 \times 21 \times 21$ grid is used for level set computations in the quarter. The volume allowed for the structure is 20% of the design domain.

In the first example, the design problem is solved without considering the molding constraint. The initial design is a block which is the same as the design domain and has no interior void. The initial Φ is a signed distance function to the six faces of the design domain. The optimization process is observed from two view directions which are shown in Figs. 8a–d and 9a–d. From these figures we can see that dramatic topology changes occurred during the optimization process. Also, we can see that although a new void cannot be nucleated right in the interior of a structure (Allaire et al. 2004), a hole can be "tunneled" through the material region in between two pieces of boundary. Therefore, compared to the situation in 2D, the optimization in 3D is topologically more flexible and less sensitive to the initial design.

The resulting optimal structure is shown in Fig. 10a. It is a framework-like structure and is hard to be manufactured using the casting process considered in the present study. A possible solution to its casting is to revise this optimal structure. However, when the structure is revised, probably its performance will be lost. If major revisions are necessary, it maybe as difficult as designing a structure from scratch.

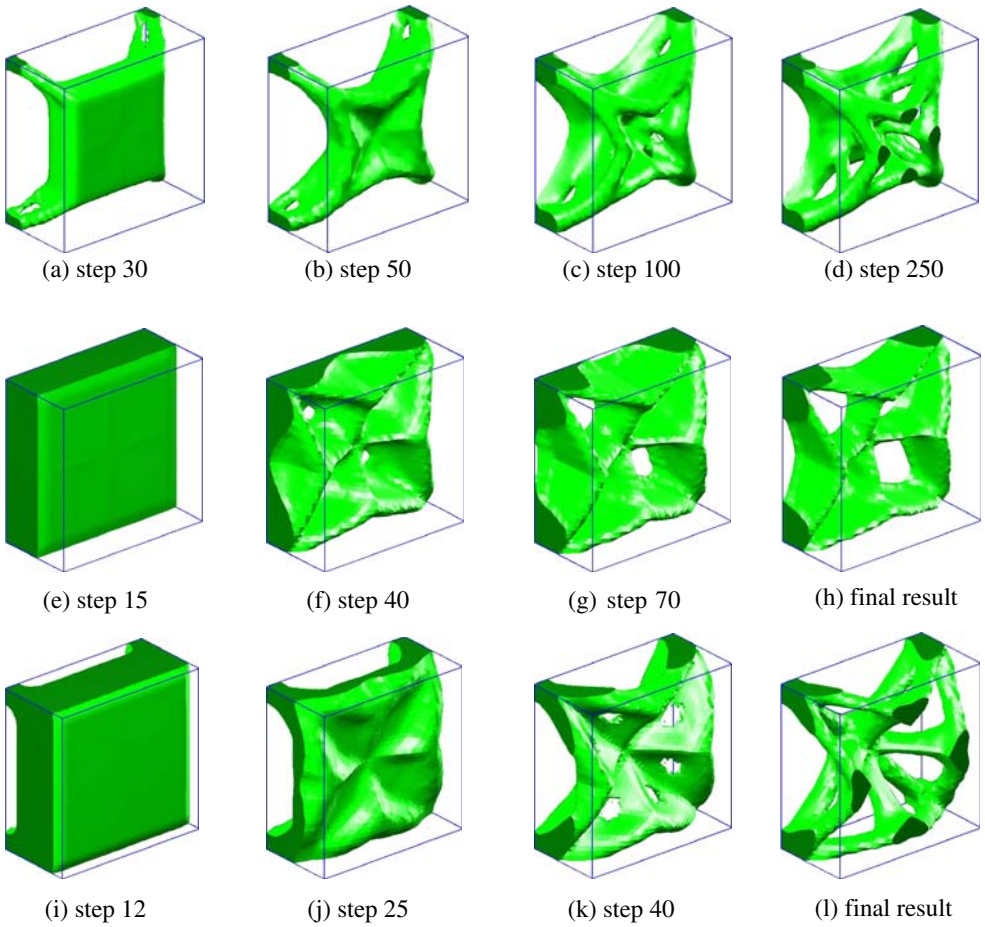

Fig. 8 Process of the optimization. **a–d** process of the optimization without considering molding constraint; **e–h** process of the optimization with molding constraint and with a pre-selected parting surface; **i–l** process of the optimization with molding constraint but without a pre-selected parting surface

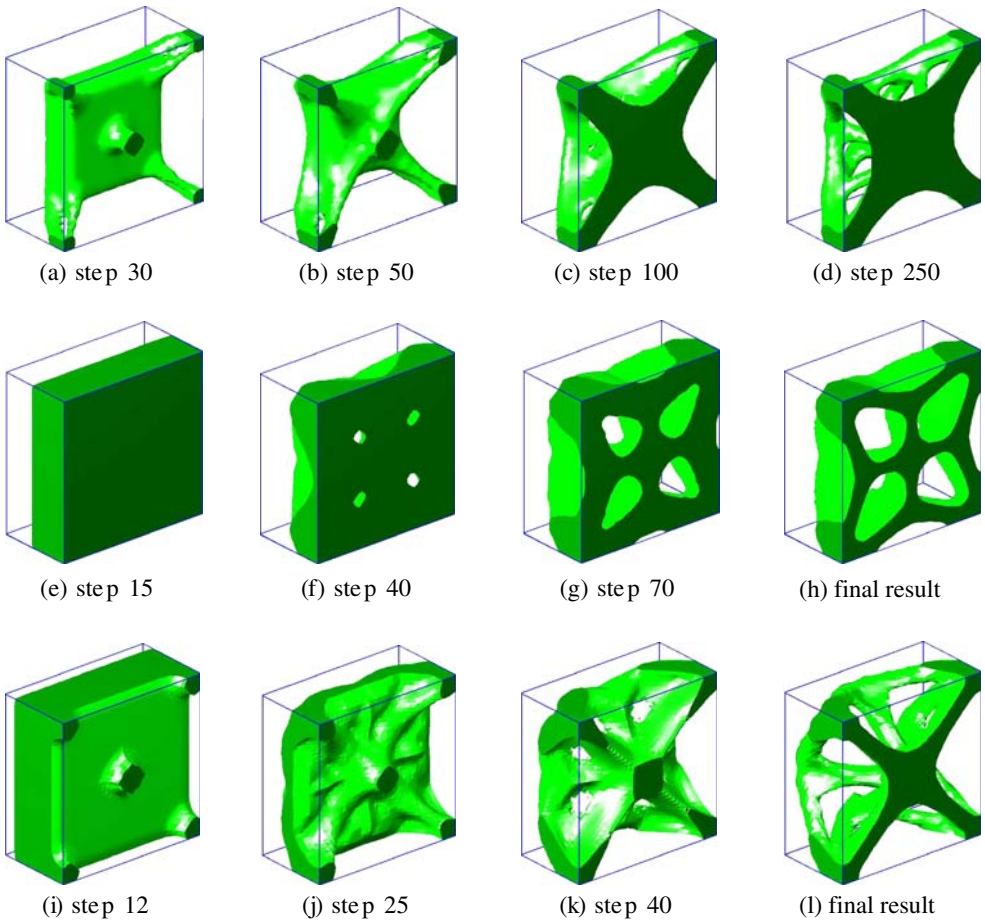

Fig. 9 Process of the optimization—another view. **a–d** process of the optimization without considering molding constraint; **e–h** process of the optimization with molding constraint and with a pre-selected parting surface; **i–l** process of the optimization with molding constraint but without a pre-selected parting surface

This situation motivated the incorporation of the molding constraint of casting process into the design optimization.

In the second example, the molding constraint is considered. The parting directions are along Z axis, and the bottom face of the design domain is pre-selected as the parting surface. The initial design is a block which is the same as the design domain. The initial Φ is a signed distance function to five faces of the design domain, with the bottom face being excluded. In other word, although the bottom face is indeed a boundary of the initial design, it is not considered as the zero level set of the initial Φ.

The optimization process is observed from two view directions that are shown in Figs. 8e–h and 9e–h. From these figures, we can see clearly that the motion of points on the

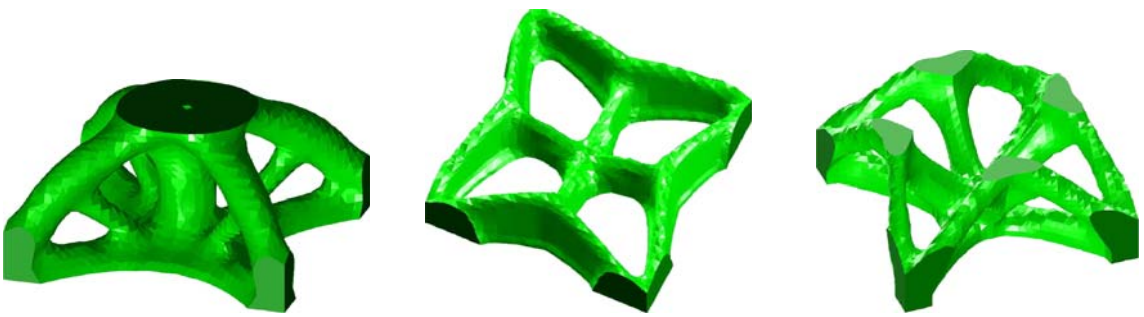

Fig. 10 The optimal structure. **a** without considering molding constraint, the volume of material is 20.27% and the compliance is 170.95; **b** with molding constraint and with a pre-selected parting surface, the volume of material is 20.00% and the compliance is 180.94; **c** with molding constraint but without a pre-selected parting surface, the volume of material is 19.97% and the compliance is 171.37

structure boundary is restricted to be along the Z axis. Such restriction of the boundary motion prevents undercuts from arising and also prevents interior void from being enclosed. The resulting optimal design of the cast part is shown in Fig. 10b. This optimal design can be manufactured with the pre-selected parting surface and parting directions using the casting process considered in our present study. The convergence history is shown in Fig. 11a.

In the third example, the parting directions are along the Z axis, but there is no pre-selected parting surface. The initial design is a block which is the same as the design domain. The initial Φ is a signed distance function to six faces of the design domain. The optimization process is observed from two view directions that are shown in Figs. 8i–l and 9i–l. From the two figures, we can see clearly that the motion of points on the structure boundary is restricted to be along the Z axis. Also, we can see that the topology of the cast part is changed when holes are "tunneled" through the material region in between two pieces of boundary. The resulting optimal structure is shown in Fig. 10c. It can be seen that the geometry of this optimal structure appears more complex than the one shown in Fig. 10b. The reason of this increased complexity of geometry is that in this example there is no pre-selected parting surface. The convergence history is shown in Fig. 11b.

In the fourth example, the parting directions are along Y axis, and the parting surface is pre-selected to be the plane which is parallel to Y and Z axis and passes through the center of the design domain, as illustrated in Fig. 12. The initial design is a block which is the same as the design domain. The initial Φ is a signed distance function to six faces of the design domain. The optimization process is observed from two view directions and are shown in Fig. 13. The resulting optimal structure is shown in Fig. 14a and one of the two same molds for casting this optimal structure is shown in Fig. 14b. Finally, the history of convergence is shown in Fig. 15 from which we can see that the convergence is quite smooth.

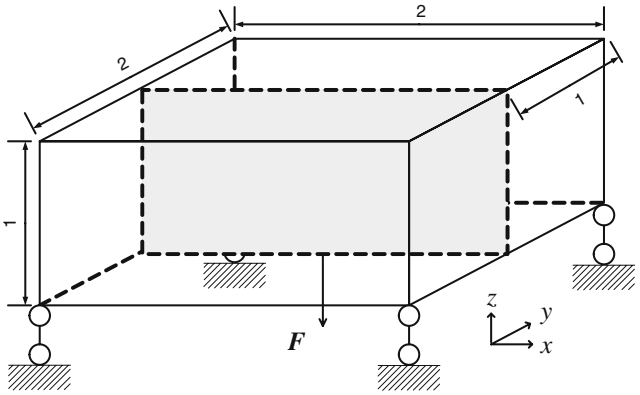

Fig. 12 The design problem of the fourth example in 3D

It can been seen from the quantitative results described in the caption of Figs. 10 and 14 that the compliance of the optimal structure obtained without considering the molding constraint is a little smaller than those obtained with molding constraint. Obviously, the compliance of the optimal structure increases when molding constraints is incorporated into the optimization.

When compared to the existing method for the optimization of cast part, especially those based on the SIMP method, the level set based method can be found to give an easier enforcement of the molding constraint. The reason is described as follows. The molding constraint is essentially a geometric type constraint. The SIMP method, however, using distribution density of material as the design variables, only gives "raster" geometry of a structure and can not directly control the geometry of a structure. Therefore, when using the SIMP method for the optimization of cast part, a lot of constraints need to be added to the optimiza-

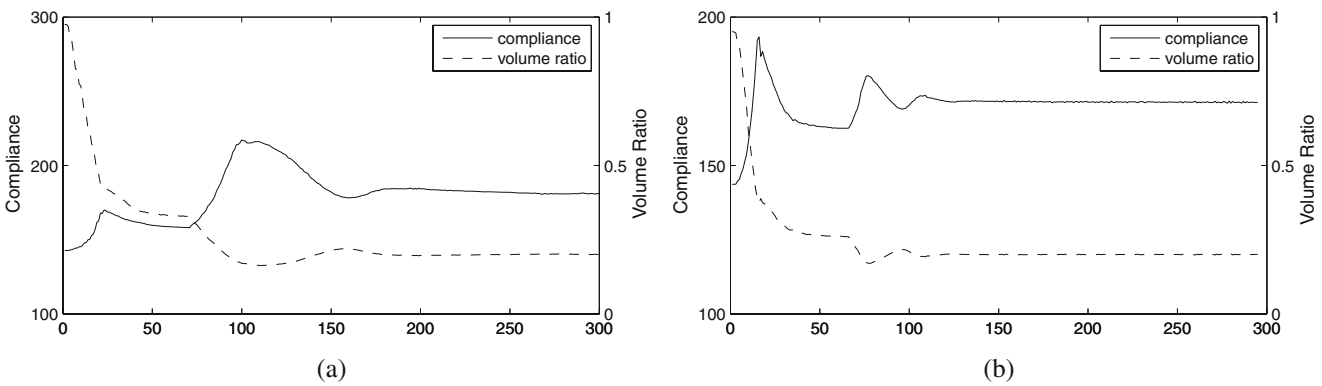

Fig. 11 The convergence history. **a** with molding constraint and with a pre-selected parting surface; **b** with molding constraint but without a pre-selected parting surface

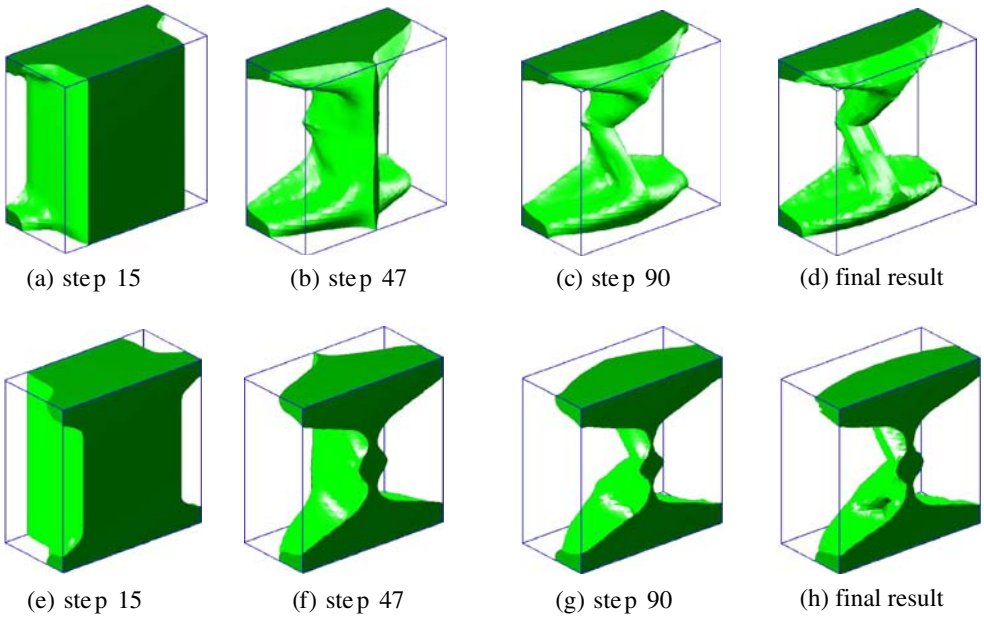

Fig. 13 Process of the optimization with molding constraint. **a**–**d** one view; **e**–**h** another view

tion problem. In the contrary, the level set method, using the free boundary of a structure as its design variable, gives direct modeling of the geometry of a structure and can give more convenient control of the geometry.

However, there also exist disadvantages of the present level set based method. As we can see from the examples in the last section, the present optimization is greatly restricted by the current level set based method, and the optimization appears as a shape optimization. It is known that void can not be nucleated by the level set method during the course of optimization. This fact motivated the integration of topological derivative (Sokolowski and Zochowski 1999) into the level set based topology optimization (Allaire and Jouve 2006; Burger et al. 2004; He et al. 2007). With such integration, the optimization can introduce voids at the positions indicated by topological derivative to decrease the objective function and to bring the design towards the feasible region, or both. If the topological derivative is not used, one usually starts the level set-based optimization with an initial design having a lot of voids. These voids can gradually be removed by the level set method, and this case is also a topology optimization. However, in the present level set based optimization of cast part, since it does not integrate the topological derivative, neither allow the initial design to have internal voids, it actually is a shape optimization, and the results obtained are only local optima. In the contrary, the SIMP method can start the optimization with an arbitrary, infeasible design, i.e. one that violates the molding constraint, and drive it gradually to a feasible design. In this aspect, the SIMP based method is more flexible than the present level set based method.

Also, with the existing SIMP based method, one can control the "length scale", more pertinent to the cast part design the "wall thickness". For a given material there typically exists a wall thickness below which solidification problems arise. So it is of practical significance to control the wall thickness during the optimization of cast part. This is not considered in the present work but should be addressed in the future work.

Finally, when the molding constraint is incorporated into the structural optimization, whether it is solved via the SIMP method or the level set method, the flexibility for delivering topology changes during the optimization will surely be reduced. In other word, the molding constraint generally shrinks the design space and may exclude the optimal solution that would be obtained without the molding

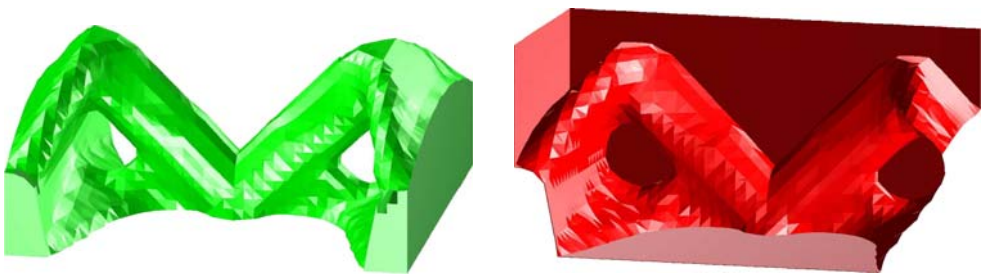

Fig. 14 The optimal structure obtained with molding constraint and the mold for casting the optimal structure. **a** the optimal structure, the volume of material is 19.99% and the compliance is 177.74; **b** the mold

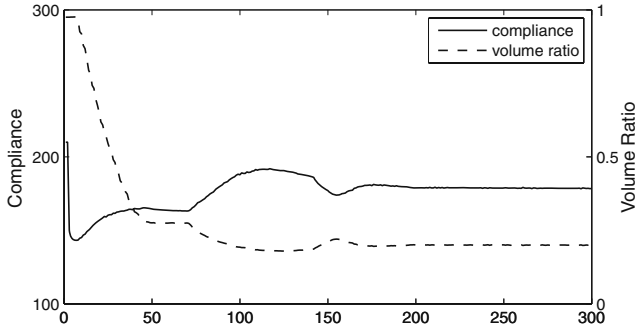

Fig. 15 The convergence history of the fourth example in 3D

constraint. In this context the topologies are generally different from that obtained without molding constraint. This fact is manifested in the aforementioned quantitative results.

9 Conclusions

This paper presents a level set based method for the optimization of cast parts. A molding condition on the design velocity is introduced to restrict the motion of free boundary during the optimization. A performance condition on the design velocity is derived based on shape derivative. Combining the two conditions, we arrive at the design velocity which is employed in the level set based topology optimization. Several numerical examples in 2D and 3D are provided.

The present method to deal with the molding constraint of casting process is a restriction method. It restrict the initial design and the motion of free boundary. If a more flexible relaxation method can be developed, it may be superior to the present restriction method. In the relaxation method, the intermediate design during the optimization process may violate the molding constraint, but the final result should satisfy the molding constraint. Also, the future work should address the issue of the control of wall thickness as aforementioned.

Acknowledgments This research work is partly supported by the Special Fund for Basic Research Work in Central Universities, the National Fundamental Research Programme of China (Grant No. 2009CB724204), the National Natural Science Foundation of China (Grant No. 50775090), and the Program for New Century Excellent Talents in University of China (Grant No. NCET-06-0639) which the authors gratefully acknowledge. The insightful comments of the reviewers' are cordially appreciated.

References

Ahn HK, Berg MD, Bose P, Cheng SW, Haplerin D, Matoušek J, Schwarzkopf O (2002) Separating an object from its cast. J Comput-aided Des 34:547–559

Allaire G, Jouve F (2006) Coupling the level set method and the topological gradient in structural optimization. In: Bendsøe MP, Olhoff N, Sigmund O (eds) IUTAM symposium on topological design optimization of structures, machines and materials, vol 137, pp 3–12

Allaire G, Jouve F, Toader AM (2002) A level-set method for shape optimization. C R Acad Sci Paris, Ser I, 334:1–6

Allaire G, Jouve F, Toader AM (2004) Structural optimization using sensitivity analysis and a level-set method. J Comput Phys 194:363–393

Baumgartner A, Harzheim L, Mettheck C (1992) SKO (soft kill option): the biological way to find an optimum structure topology. Int J Fatigue 14:387–393

Bendsøe MP (1989) Optimal shape design as a material distribution problem. Struct Optim 1:193–202

Bendsøe MP, Sigmund O (2003) Topology optimization: theory, methods and applications. Springer, Berlin

Burger M, Hackl B, Ring W (2004) Incorporating topological derivatives into level set methods. J Comput Phys 194:344–362

Ebrahimi SA, Tortorelli DA, Dantzig JA (1997) Sensitivity analysis and nonlinear programming applied to investment casting design. Appl Math Model 21:113–123

Fu MW, Nee AYC, Fuh JYH (2002) The application of surface visibility and moldability to parting line generation. J Comput-aided Des 34:469–480

Harzheim L, Graf G (1995) Optimization of engineering components with the sko method. In: The ninth international conference on vehicle structural mechanics and CAE, pp 235–243

Harzheim L, Graf G (2002) Topshape: an attempt to create design proposals including manufacturing constraints. Int J Veh Des 28:389–408

Harzheim L, Graf G (2005) A review of optimization of cast parts using topology optimization: I—topology optimization without manufacturing constraints. Struct Multidiscipl Optim 30:491–497

Harzheim L, Graf G (2006) A review of optimization of cast parts using topology optimization: II—topology optimization with manufacturing constraints. Struct Multidiscipl Optim 31:388–399

He L, Kao CY, Osher S (2007) Incorporating topological derivatives into shape derivative based level set methods. J Comput Phys 225:891–909

Leiva JP, Watson BC, Kosaka I (1999) Modern structural optimization concepts applied to topology optimization. In: 40th AIAA/ASME/ASCE/AHS/ASC structures, structural dynamics, and material conference, St. Louis, 12–15 April 1999

Leiva JP, Watson BC, Kosaka I (2004a) An analytical bi-directional growth parameterization to obtain optimal castable topology designs. In: 10th AIAA/ISSMO symposium on multidisciplinary analysis and optimization, Albany, 30 August–1 September 2004

Leiva JP, Watson BC, Kosaka I (2004b) An analytical directional growth topology parameterization to enforce manufacturing requirements. In: 45th AIAA/ASME/ASCE/AHS/ASC structures, structural dynamics, and material conference, Palm Springs

Lewis RW, Manzari MT, Gethin DT (2001) Optimal riser design for metal castings. Metall Mater Trans B 18:392–417

Li WS, Martin RR, Langbein FC (2007) Generating smooth parting lines for mold deisgn for meshes. In: ACM symposium on solid and physical modeling, Beijing, pp 193–204, 4–6 June 2007

Majhi JP, Gupta P, Janardan R (1999) Computing a flattes, undercut-free parting line for a convex polyhedron, with application to mold design. Comput Geom Theor Appl 13(4):229–252

Mattheck C (1990) Design and growth rule for biological structures and their application in engineering. Fatigue Fract Eng Mater Struct 13:535–550

Morthland TE, Byrne PE, Tortorelli DA, Dantzig JA (1995) Optimal riser design for metal castings. Metall Mater Trans B 26:871–885

Nocedal J, Wright SJ (1999) Numerical optimization. Springer, New York

Osher S, Fedkiw R (2002) Level set methods and dynamic implicit surfaces. Springer, New York

Osher S, Santosa F (2001) Level-set methods for optimization problems involving geometry and constraints: frequencies of a two-density inhomogeneous drum. J Comput Phys 171:272–288

Osher S, Sethian JA (1988) Front propagating with curvature dependent speed: algorithms based on Hamilton-Jacobi formulations. J Comput Phys 78:12–49

Peng DP, Merriman B, Osher S, Zhao HK, Kang M (1999) A PDE-based fast local level set method. J Comput Phys 155:410–438

Ravi B, Srinivasan MN (1990) Decision criteria for computer-aided parting surface deisgn. Comput-aided Des 22(1):11–17

Rozvany GIN, Zhou M, Birker T (1992) Generalized shape optimization without homogenization. Strut Optim 4:250–254

Sethian JA (1999) Level set methods and fast marching methods: evolving interfaces in computational geometry, fluid mechanics, computer vision, and materials science. Cambridge monographs on applied and computational mathematics, 2nd edn. Cambridge University Press, Cambridge

Sethian JA, Wiegmann A (2000) Structural boundary design via level set and immersed interface methods. J Comput Phys 163:489–528

Sokolowski J, Zochowski A (1999) On the topological derivative in shape optimization. SIAM J Control Optim 37:1251–1272

Sussman M, Smereka P, Osher S (1994) A level-set approach for computing solutions to incompressible two-phase flow. J Comput Phys 114:146–159

Tavakoli R, Davami P (2008) Optimal riser design in sand casting process by topology optimization with simp method i: Poisson approximation of nonlinear heat transfer equation. Struct Multidiscipl Optim 36:193–202

Tortorelli DA, Tiller MM, Dantzig JA (1994) Optimal design of nonlinear parabolic systems. Part i: fixed spatial domain with applications to process optimization. Comput Methods Appl Mech Eng 113:141–155

Wang MY, Wang XM, Guo DM (2003) A level set method for structural topology optimization. Comput Methods Appl Mech Eng 192:227–246

Ye JC, Bresler Y, Moulin P (2002) A self-referencing level-set method for image reconstruction from sparse Fourier samples. Int J Comput Vis 50:253–270

Zhou M, Shyy YK, Thomas HL (2001) Topology optimization with manufacturing constraints. In: 4th world congress of structural and multidisciplinary optimization, Dalian